

Recombinant adenoviruses expressing apoptin suppress the growth of MCF-7 breast cancer cells and affect cell autophagy

SHUANG CHEN¹⁻³, YI-QUAN LI^{1,2,4}, XUN-ZHE YIN^{2,4}, SHAN-ZHI LI^{2,4}, YI-LONG ZHU^{2,4},
YUAN-YUAN FAN², WEN-JIE LI², YING-LI CUI², JIN ZHAO², XIAO LI^{2,4,5},
QING-GAO ZHANG^{1,6} and NING-YI JIN^{1,2,4,5}

¹Medical College, Yanbian University, Yanji, Jilin 133002; ²Laboratory of Molecular Virology and Immunology, Institute of Military Veterinary Medicine, Academy of Military Medical Science, Changchun, Jilin 130122; ³School of Medical Inspection, Jilin Medical University, Jilin, Jilin 132013;

⁴Academician Workstation of Jilin Province, Changchun University of Chinese Medicine, Changchun, Jilin 130021;

⁵Jiangsu Co-Innovation Center for Prevention and Control of Important Animal Infectious Diseases and Zoonoses, Yangzhou, Jiangsu 225009; ⁶Medical College, Dalian University, Dalian, Liaoning 116622, P.R. China

Received July 26, 2018; Accepted February 25, 2019

DOI: 10.3892/or.2019.7077

Abstract. Autophagy and apoptosis both promote cell death; however, the relationship between them is subtle, and they mutually promote and antagonize each other. Apoptin can induce apoptosis of various tumor cells; however, tumor cell death is not only caused by apoptosis. Whether apoptin affects tumor cell autophagy is poorly understood. Therefore, the present study aimed to explore the potential mechanisms underlying the effects of apoptin using recombinant adenoviruses expressing apoptin. Reverse transcription-quantitative polymerase chain reaction, immunoblotting, flow cytometry, fluorescence microscopy and proteomics analyses revealed that apoptin could induce autophagy in MCF-7 breast cancer cells. The results also suggested that apoptin affected autophagy in a time- and dose-dependent manner. During the early stage of apoptin stimulation (6 and 12 h), the expression levels of autophagy pathway-associated proteins, including Beclin-1, microtubule-associated protein 1A/1B-light chain 3, autophagy-related 4B cysteine peptidase and

autophagy-related 5, were significantly increased, suggesting that apoptin promoted the upregulation of autophagy in MCF-7 cells. Conversely, after 12 h of apoptin stimulation, the expression levels of apoptosis-associated proteins were decreased, thus suggesting that apoptosis may be inhibited. Therefore, it was hypothesized that apoptin may enhance autophagy and inhibit apoptosis in MCF-7 cells at the early stage. In conclusion, apoptin-induced cell death may involve both autophagy and apoptosis. The induction of autophagy may inhibit apoptosis, whereas apoptosis may inhibit autophagy; however, occasionally both pathways operate at the same time and involve apoptin. This apoptin-associated selection between tumor cell survival and death may provide a potential therapeutic strategy for breast cancer.

Introduction

Apoptin was originally identified as an apoptosis-inducing protein derived from chicken anemia virus (CAV), which is a single-stranded DNA virus of the *Gyrovirus* genus (1). The CAV genome contains three partially overlapping open reading frames encoding viral proteins from a single polycistronic mRNA: VP1 (capsid protein), VP2 (protein phosphatase, scaffold protein) and the death-inducing protein VP3 (2). The expression of VP3 alone has been reported to be sufficient to trigger cell death in chicken lymphoblastoid T cells and myeloid cells, but not in chicken fibroblasts; therefore, this protein has been renamed apoptin (3). The gene encoding apoptin was among the first tumor-selective anticancer genes to be isolated, and has become a focus of cancer research due to its ability to induce apoptosis of various human tumor cells, including melanoma, lymphoma, colon carcinoma and lung cancer, while leaving normal cells relatively unharmed (4-7). It may be hypothesized that apoptin senses an early event in oncogenic transformation and induces cancer-specific

Correspondence to: Dr Ning-Yi Jin, Laboratory of Molecular Virology and Immunology, Institute of Military Veterinary Medicine, Academy of Military Medical Science, 66 Liuying West Road, Jingyue Economic and Technological Development Zone, Changchun, Jilin 130122, P.R. China
E-mail: skyllee6226@163.com

Dr Qing-Gao Zhang, Medical College, Dalian University, 10 Xuefu Street, Dalian, Liaoning 116622, P.R. China
E-mail: zqg0621@ybu.edu.cn

Key words: apoptin, autophagy, breast cancer, microtubule-associated protein 1A/1B-light chain 3, autophagy pathway

apoptosis, regardless of tumor type; therefore, it represents a potential future anticancer therapeutic agent.

The length and viability of human telomerase reverse transcriptase (hTERT) are associated with cell senescence and immortalization. Telomerase is a ribonucleoprotein that can process telomere repeats (TTAGGG) at the ends of chromosomes (8). Telomerase activity is regulated by the signal transduction system and the apoptotic pathway, and its activity is a marker of immature cell differentiation and immortalization. The hTERT promoter is inactive in most normal cells; however, it exhibits high activity in several types of human cancer (9). Previous studies revealed that targeting to tumor cells and efficient expression of the protein of interest is also dependent on the high efficiency and specificity of the hTERT promoter, thus providing novel prospects for tumor therapy (10,11). In our previous study, using the characteristics of apoptin and the hTERT promoter, a tumor-specific replication recombinant adenovirus expressing apoptin (Ad-Apoptin-hTERTp-E1a; Ad-VT) was constructed (12), which allows the adenovirus to specifically replicate in tumor cells, and enables the apoptin protein to be expressed in a large amount in tumor cells, thereby playing an effective role in tumor cell death. Our previous studies have demonstrated the marked tumor-killing effect of the recombinant adenovirus on various tumor cells (13-16).

Autophagy, which is described as 'self-eating', constitutes a self-degradation process, and is a critical mechanism underlying the cytoprotection of eukaryotic cells (17). It is a catabolically driven process whereby stressed cells form cytoplasmic, double-layered, crescent-shaped membranes, known as phagophores, which mature into complete autophagosomes. The autophagosomes engulf long-lived proteins and damaged cytoplasmic organelles, in order to provide cellular energy and building blocks for biosynthesis (18). However, in the context of cancer, autophagy appears to serve an ambiguous role. In association with apoptosis, autophagy can act as a tumor suppressor. Conversely, defects in autophagy, alongside abnormal apoptosis, may trigger tumorigenesis and therapeutic resistance (19,20).

The role of autophagy as an alternative cell death mechanism remains a controversial issue. It was previously reported that dying cells exhibit autophagic vacuolization (21), which led to the suggestion that cell death is mediated by autophagy. However, to the best of our knowledge, there is no concrete evidence that autophagy is a direct mechanism used to execute cell death. Numerous studies have suggested that autophagy may lead to apoptosis or necroptosis as a result of a failure to adapt to starvation (22-24). Therefore, autophagy may constitute an adaptive response to counteract cell death under lethal stress conditions, rather than a cell death mechanism (21,25). The autophagic response is activated in response to ATP depletion to restore the metabolic state and to prevent necroptosis (26-28). In addition, autophagy ensures cell metabolism, promotes tumor cell survival, and prevents cancer cells from accumulating dysfunctions (29). Therefore, inhibition of autophagy could induce a metabolic crisis that leads to the induction of necroptosis (30,31).

The recombinant adenovirus Ad-VT can specifically kill tumor cells; however, it remains to be determined as to whether Ad-VT affects another form of programmed

cell death from apoptosis, such as autophagy. In addition, if it does affect autophagy, it is unclear how. In the present study, MCF-7 breast cancer cells and MCF-10A normal breast epithelial cells were used. The levels of autophagy were detected using monodansylcadaverine (MDC). Western blotting and reverse transcription-quantitative polymerase chain reaction (RT-qPCR) were used to assess the expressions levels of autophagy-associated proteins, including Beclin-1, microtubule-associated protein 1A/1B-light chain 3 (LC3), autophagy-related 4B cysteine peptidase (ATG4b), autophagy-related 5 (ATG5), P62 and BIF-1. Cell morphology was observed by transmission electron microscopy (TEM) following infection with recombinant adenoviruses expressing apoptin. A proteomics experiment was also conducted to observe alterations in the levels of autophagy pathway proteins. The results revealed that the recombinant adenoviruses expressing apoptin altered autophagy in the MCF-7 breast cancer cell line, but had no effect on MCF-10A normal mammary epithelial cells. These findings suggested that autophagy in MCF-7 cells may exert protection against the cell death-inducing effects of apoptin.

Materials and methods

Cells and viruses. The MCF-7 human breast cancer cells and MCF-10A human normal mammary epithelial cells were cryopreserved cells purchased from the Shanghai Institute of Biology Cell Bank (Shanghai, China). MCF-7 cells were maintained in RPMI 1640 medium supplemented with 10% fetal bovine serum (FBS), 50 U/ml penicillin and 50 U/ml streptomycin at 37°C in an atmosphere containing 5% CO₂. MCF-10A cells were maintained in Dulbecco's modified Eagle's medium supplemented with 10% FBS, 50 U/ml penicillin and 50 U/ml streptomycin at 37°C in an atmosphere containing 5% CO₂. All reagents for cell culture were purchased from HyClone; GE Healthcare Life Sciences (Logan, UT, USA).

Recombinant adenoviruses Ad-VT, Ad-Apoptin (Ad-VP3) and Ad-MOCK were constructed and preserved in our laboratory (Laboratory of Molecular Virology and Immunology, Institute of Military Veterinary Medicine, Academy of Military Medical Science, Changchun, China) (Fig. 1) (12).

Cell viability assay. MCF-7 and MCF-10A cells were seeded in 96-well plates (5x10³ cells/well). After 24 h of culture, the cells were infected with various concentrations of the recombinant adenoviruses [50, 100 and 200 multiplicity of infection (MOI)], and blank control wells were set. After 6, 12, 24, and 48 h, 10 µl WST-1 solution (cell proliferation assay reagent; cat. no. 11644807001; Roche Applied Science, Mannheim, Germany) was mixed with 100 µl cell culture medium and was added to each well; cells were then incubated at 37°C in an atmosphere containing 5% CO₂ for 1 h and 20 min. Subsequently, absorbance was measured at 450 nm. Cell viability was calculated as follows: Cell viability = 100 x (absorbance of virus-treated wells/absorbance of control wells).

Measurement of apoptosis by flow cytometry. MCF-7 and MCF-10A cells were infected with the recombinant adenoviruses (100 MOI). After 24 h, the cells (2x10⁵) were harvested,

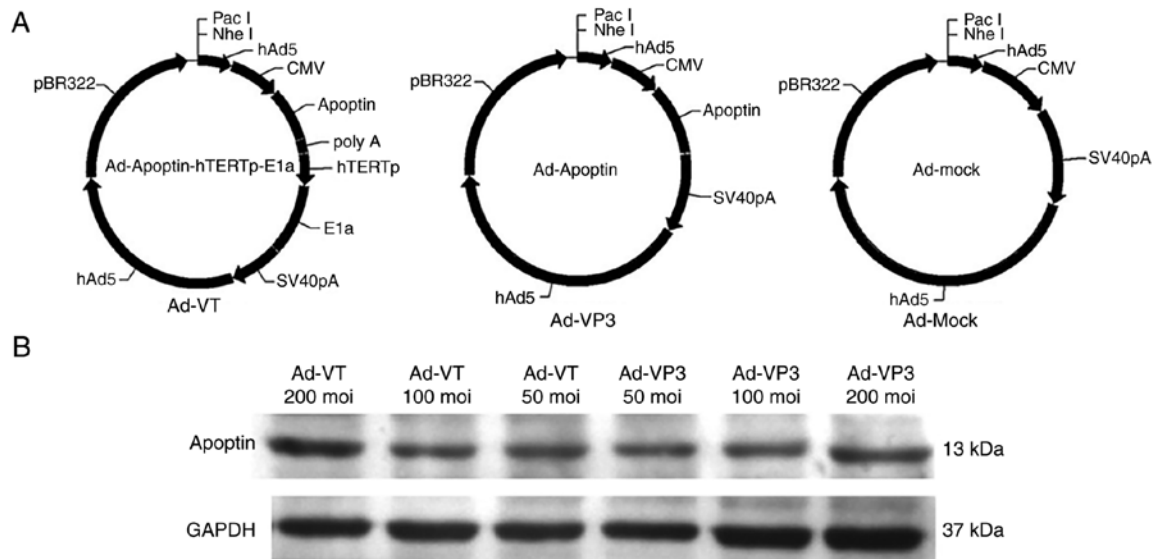


Figure 1. Schematic diagram of the three recombinant adenovirus vectors constructed using shuttle vectors. (A) Ad-VT, Ad-VP3 and Ad-MOCK. (B) MCF-7 cells were infected with Ad-VT and Ad-VP3 at 50, 100 and 200 MOI, and the protein expression levels of apoptin were detected. Ad-VP3, Ad-Apoptin; Ad-VT, Ad-Apoptin-hTERTp-E1a; MOI, multiplicity of infection.

resuspended in binding buffer and stained with fluorescein isothiocyanate (FITC)-labeled Annexin V (Annexin V-FITC Apoptosis Detection kit; BioVision, Inc., Milpitas, CA, USA), according to the manufacturer's protocol. To exclude late apoptotic and necrotic cells, propidium iodide (PI; 50 $\mu\text{g}/\text{ml}$) was added to the FITC-Annexin V-stained samples and incubated at room temperature for 20 min. The samples were then examined by flow cytometry (FACSCalibur; BD Biosciences, Franklin Lakes, NJ, USA) for apoptosis analysis (Cell Quest Pro 5.2.1; BD Biosciences).

3-Methyladenine (3-MA; cat. no. M9281; Sigma-Aldrich; Merck KGaA, Darmstadt, Germany) was dissolved in PBS and stored at -20°C . Prior to use, 3-MA solution was heated to 56°C to completely dissolve it, and was then added to MCF-7 and MCF-10A cell culture media at a final concentration of 50 mmol/l and incubated for 2 h. Following 3-MA treatment, MCF-7 cells underwent flow cytometry and western blotting, whereas MCF-10A cells underwent flow cytometry.

Cell cycle analysis. Cells were infected with recombinant adenoviruses (100 MOI) for 24 h. After washing with PBS, the cells were harvested and fixed overnight in 70-80% ethanol. The next day, cells were washed with 1X PBS and were centrifuged at $175 \times g$ for 10 min at room temperature, after which, the supernatant was discarded. Cells were then mixed with 0.09% NaN₃ Stain Buffer (2% FBS), washed and centrifuged at $175 \times g$ for 10 min at room temperature, and the supernatant was discarded. Finally, 500 μl PI/RNase (PI/RNase Staining Buffer; cat. no. 550825; BD Pharmingen; BD Biosciences) staining solution was used to stain the cells for 1 h at room temperature. Flow cytometry was performed using a FACSCalibur instrument and Cell Quest Pro 5.2.1 software.

MDC detection. Cells (2×10^5 MCF-7 cells) were placed in each well of 6-well plates for 24 h. Following infection with recombinant adenoviruses (100 MOI) for 6 h, autophagic vacuoles were labeled with 0.05 mmol/l MDC (cat. no. 30432;

Sigma-Aldrich; Merck KGaA) in cell culture medium at 37°C for 15 min. The cells were then washed three times with PBS. Autophagic vacuoles in MCF-7 cells were observed under a fluorescence microscope (BX-60; Olympus Corporation, Tokyo, Japan) and analyzed using MetaMorph 6.2.6 software (Molecular Devices, LLC, Sunnyvale, CA, USA). Notably, >5 fluorescent spots were considered to indicate positive fluorescence, and 100 cells were counted to calculate the rate of autophagy.

Enhanced green fluorescent protein-LC3 plasmid (p-EGFP-LC3) transfection. MCF-7 cells ($2 \times 10^5/\text{well}$) in 12-well plates with microscope cover glasses (Thermo Fisher Scientific, Inc., Waltham, MA, USA) were transfected with 5 μg pEGFP-LC3 (2.92 $\mu\text{g}/\mu\text{l}$; cat. no. 24920; Addgene, Inc., Cambridge, MA, USA) using 5 μl X-tremeGENE™ HP DNA Transfection Reagent (cat. no. 6366236001; Roche Applied Science) for 24 h. Subsequently, cells were fixed with 4% paraformaldehyde in PBS and cellular images were obtained under a fluorescence microscope (BX-60; Olympus Corporation) using MetaMorph 6.2.6 software.

TEM. TEM is considered the most reliable approach to monitor autophagy (32). MCF-7 cells were cultured in 6-well plates for 24 h and infected with recombinant adenoviruses (100 MOI) for 6 h. Cells were then collected and cells were fixed in 2.5% glutaraldehyde at 4°C for 8 h. Ultrathin sections (50 nm) were cut using an ultramicrotome, stained with 2% (w/v) uranyl acetate for 15 min and with lead citrate for 10 min at room temperature, and examined under a JEM-100cxII electron microscope (JEM-1010; JEOL, Ltd., Tokyo, Japan).

RNA isolation and RT-qPCR analysis. RNA was isolated from cells using TRIzol® (Invitrogen; Thermo Fisher Scientific, Inc.). RT was performed using RT reagents (M-MLV Reverse Transcriptase; cat. no. M1705; Promega Corporation, Madison, WI, USA), as follows: 42°C for 50 min followed by 75°C for

15 min. The mRNA expression levels of human LC3, Beclin-1, GAPDH and P62 were measured by qPCR using the GoTaq qPCR Master Mix (cat. no. A6002; Promega Corporation) on a StepOne Real-Time PCR System (7500 Real-Time PCR system; Applied Biosystems; Thermo Fisher Scientific, Inc.). All protocols were performed according to the manufacturers' protocols. The PCR reaction conditions were as follows: 95°C for 5 min followed by 40 cycles at 95°C for 15 sec, 60°C for 30 sec and 72°C for 30 sec, and a final extension step at 72°C for 10 min. The primers used in the present study were as follows (5'-3'): Beclin-1, forward (F) CCGTGGTAACCTTGTTCATCC, reverse (R) GCTCTGTCTTCAGCGACTTCC; LC3-II, F AATAGAAGGCGCTTACAG, R GACAATTTCATCCCGAAC; P62, F GGACAAACGGCTCACTCT, and R TGCCAGTTCCTCATTCT; and GAPDH, F AACGGA TTTGGTCGTATTG and R GGAAGATGGTGATGGGATT. The $2^{-\Delta\Delta C_q}$ method was used to quantify the PCR results (33).

Cell extracts and western blotting. Certain autophagy-associated proteins were detected by immunoblotting. Briefly, whole cell lysates were prepared from treated MCF-7 cells at the indicated time points using 1X radioimmunoprecipitation assay (RIPA) buffer (cat. no. P0013; Beyotime Institute of Biotechnology, Haimen, China), according to the manufacturer's protocol. In addition, 10 mM phenylmethanesulfonyl fluoride (PMSF; cat. no. ST506-2; Beyotime Institute of Biotechnology) was generated and stored at -20°C. Prior to cell lysis, PMSF was added RIPA buffer to a final concentration of 1 mM PMSF. Four-fold volume of RIPA cleaved cells. Cleaved cells were sonicated at 4°C (15 cycles, 30 sec/cycle, 60 Hz) using a Bioruptor UCD-300 device (Diagenode SA, Seraing, Belgium). The protein concentration was measured using the bicinchoninic acid protein assay (cat. no. P0010s; Beyotime Institute of Biotechnology). Proteins were loaded into each lane and separated by 10% SDS-PAGE, and were then electrotransferred onto nitrocellulose (NC) membranes (0.45 μ m NC; cat. no. 10600002; Amersham; GE Healthcare, Chicago, IL, USA). The membranes were blocked with 5% non-fat dried milk in PBS supplemented with 0.1% Tween 20 (PBST; cat. no. 170653; Bio-Rad Laboratories, Inc., Hercules, CA, USA) at room temperature for 2 h, and were then incubated overnight with the corresponding primary antibodies (1:1,000) at 4°C overnight. The blots were then incubated with a secondary antibody (1:2,000) for 2 h at room temperature after three washes with PBST. The membranes were further washed three times with PBST before being developed using Clarity Western ECL Blotting Substrate (cat. no. 32209; Pierce; Thermo Fisher Scientific, Inc.). Images were collected following development of photographic paper (X-OMAT BT Film; cat. no. 045602811; Carestream Health, Inc., Rochester, NY, USA).

Antibodies for western blotting. The following primary antibodies were used: Rabbit anti-GAPDH (cat. no. 5174), rabbit anti-B-cell lymphoma 2 (Bcl-2; cat. no. 3498), rabbit anti-Bcl-2-associated X protein (Bax; cat. no. 5023), rabbit anti-LC3 (cat. no. 12741), rabbit anti-Beclin-1 (cat. no. 3495), rabbit anti-ATG4b (cat. no. 13507), rabbit anti-BIF-1 (cat. no. 4467), rabbit anti-ATG5 (cat. no. 12994), and rabbit anti-tubulin (cat. no. 2148) (all from Cell Signaling Technology, Inc.,

Danvers MA, USA), and rabbit anti-sqstm1/P62 (cat. no. p0067; Sigma-Aldrich; Merck KGaA). The following secondary antibody was used: Peroxidase-conjugated goat anti-rabbit immunoglobulin G (H+L) (cat. no. ZB2301; OriGene Technologies, Inc., Beijing, China).

Total (phospho) proteome workflow. Approximately 2×10^4 adenovirus-infected MCF-7 cells were rinsed with PBS and lysed with RIPA buffer. Cells were collected in a 1.5 ml centrifuge tube and were centrifuged at 4°C and 1,950 x g for 5 min. The supernatant was discarded and 4-fold volume RIPA [8 M urea + phosphatase inhibitor (10X)] was added to the sample, according to the volume of the precipitate. Cells were then sonicated on ice (20 kHz; ultrasound for 1 sec, stop for 2 sec; total, 60 sec), maintained for 20 min at 4°C and centrifuged at 16,000 x g for 5 min. Proteins in the supernatant were assessed using the Bradford reagent. After protein quantification, 1 mg protein solution was treated with dithiothreitol (10 mM; cat. no. 0281; Amresco, LLC, Solon, OH, USA) in a water bath was 30 min. Subsequently, iodoacetamide (20 mM; cat. no. I1149; Sigma-Aldrich; Merck KGaA) was added at room temperature was 30 min and alkylation was carried out. After alkylation, the protein solution was centrifuged for 15 min at 14,000 x g, and the waste liquid was discarded. The protein sample was washed with 8 M urea, centrifuged at 14,000 x g for 15 min and the waste liquid was discarded; this step was repeated twice. For enzymatic hydrolysis, 50 mM sodium bicarbonate and 1.6 μ g trypsin (mass ratio 1/50) were added, the sample was agitated and digestion was conducted at 37°C for 16 h. For peptide segment collection, the sample was centrifuged for 10 min at 14,000 x g and the peptide solution was collected; subsequently, 200 μ l high-performance liquid chromatography- H_2O was added to the solution, which was centrifuged for a further 10 min at 14,000 x g and this second peptide solution was collected. Finally, the collected peptide segment solutions were combined, freeze-dried and stored at -80°C.

(Phospho) proteomic data mining. The choice of database was based on the required species, and the completeness and reliability of the database annotation. In the present study, the Uniprot database (www.uniprot.org) was used. MaxQuant 1.5.8.3 software (Max-Planck-Institute of Biochemistry, Planegg, Germany) was used to retrieve and quality control the tandem mass spectrum, remove contaminating proteins and conduct reverse decoy database analysis, normalize data and provide log₂ values. The numerical values were inputted directly into The R Project for Statistical Computing (version 3.5.1; www.r-project.org/), and the pheatmap function was selected for classification analysis, resulting in the generation of a thermal graph and hierarchical clustering. The pathways associated with the differential proteins were determined using Kyoto Encyclopedia of Genes and Genomes (KEGG; www.kegg.jp/kegg) pathway analysis.

Statistical analysis. Statistical analysis was conducted using data from at least three independent experiments. SPSS 20.0 (SPSS, Inc., Chicago, IL, USA) or SigmaStat 3.5 (Systat Software, Inc., San Jose, CA, USA) were used for statistical analysis. The results were statistically analyzed by

Student's t-test or one-way analysis of variance (ANOVA); when one-way ANOVA results were $P < 0.05$, further multiple comparisons were performed using the Student-Newman-Keuls test. $P < 0.05$ was considered to indicate a statistically significant difference.

Results

Antiproliferative effect of recombinant adenoviruses on MCF-7 and MCF-10A cells. The antiproliferative activity of recombinant adenoviruses on MCF-7 and MCF-10A cells was investigated using the WST-1 assay, which is a sensitive colorimetric assay to determine cell viability that measures dehydrogenase activity in living cells (Fig. 2). Post-infection with Ad-VT, Ad-VP3 and Ad-MOCK for 6, 12, 24 and 48 h, MCF-7 cell proliferation was inhibited in a time- and dose-dependent manner (Fig. 2A and C); however, the recombinant adenoviruses exhibited no obvious inhibitory effect on MCF-10A cells (Fig. 2A). In addition, Annexin V-FITC/PI double staining was conducted to detect the levels of apoptosis (Fig. 3A-D). The apoptotic rate of MCF-7 tumor cells was significantly increased in response to the recombinant adenoviruses Ad-VT and Ad-VP3 over 24 h (Fig. 3A and C). When the recombinant adenoviruses Ad-VT or Ad-VP3 were combined with the autophagy inhibitor 3-MA, the apoptotic rate of tumor cells was increased compared with when cells were infected with Ad-VT or Ad-VP3 alone; therefore, it was suggested that inhibition of autophagy may increase the apoptosis of MCF-7 cells infected with recombinant adenoviruses over 24 h (Fig. 3A and C). In addition, no significant alterations in apoptosis were detected in MCF-10A normal human breast cells (Fig. 3B and D). In the present study, the early stage of apoptosis (24 h) was selected, which was not very strong; in order to more clearly discover the effect of autophagy. The results revealed that the addition of an autophagy inhibitor increased the rate of apoptosis, and it was hypothesized that apoptin-induced autophagy in the early stage of apoptosis may inhibit the occurrence of apoptosis.

Inhibition of autophagy increases the Bax/Bcl-2 ratio. Following inhibition of autophagy with 3-MA, MCF-7 cells were infected with Ad-VT and Ad-VP3 at 100 MOI for 12 h, and the expression levels of apoptosis-associated proteins Bcl-2 and Bax were detected by western blotting. As shown in Fig. 3E, the autophagy inhibitor 3-MA was used to investigate the association between autophagy and apoptosis following infection of MCF-7 cells with recombinant adenoviruses. Compared with in the blank control group, the expression levels of Bcl-2 were decreased in the Ad-VP3, Ad-VT, Ad-VP3 + 3-MA and Ad-VT + 3-MA groups, and it was suggested that Ad-VP3 and Ad-VT gradually induced apoptosis at 12 h. The expression levels of Bcl-2 in the Ad-VP3 + 3-MA and Ad-VT + 3-MA groups were significantly lower than in the Ad-VP3 and Ad-VT groups ($P < 0.01$), thus indicating that inhibition of autophagy can further induce apoptosis of tumor cells induced by the recombinant adenoviruses. In addition, compared with in the Ad-VP3 and Ad-VT groups, the expression levels of the proapoptotic protein Bax were significantly increased in the Ad-VP3 + 3-MA and Ad-VT + 3-MA groups ($P < 0.01$ and $P < 0.05$), and the ratio of Bax/Bcl-2 was increased. These

findings indicated that inhibition of autophagy, alongside infection with the recombinant adenoviruses, promoted the occurrence of apoptosis at 12 h. This early autophagy may protect MCF-7 cells from apoptosis.

Recombinant adenoviruses induce cell cycle arrest at G₁ phase in MCF-7 cells. The cell cycle is a repeating series of events that take place in a cell leading to its division and DNA replication, thus resulting in the production of two daughter cells. Disturbance of the cancer cell cycle may inhibit cell growth and activate autophagy. To explore the potential tumor suppressive mechanism of recombinant adenoviruses, their effects on cell cycle progression were determined. Representative results for MCF-7 cells infected with the control and recombinant adenoviruses are shown in Fig. 3F. Flow cytometry revealed that, compared with in the control group (uninfected cells), Ad-VT infection significantly decreased the number of MCF-7 human breast cancer cells in G₂/M phase after 24 h (from 9.93 to 0.88%; $P < 0.01$; Fig. 3F), and it was hypothesized that Ad-VT may arrest MCF-7 cells at a certain cell cycle phase. Notably, it was observed that cells infected with Ad-VT and Ad-VP3 were delayed in S phase; however, this was not significant. In addition, the amount of Ad-VT-infected cells in the G₁ phase was higher. Therefore, it was suggested that Ad-VT infection for 24 h may block MCF-7 cells in G₁ phase, whereas Ad-VP3 and Ad-MOCK had no effect on the proportion of cells in G₁ phase.

Recombinant adenoviruses induce autophagy in MCF-7 cells. Autophagy is a lysosomal degradation process for cytoplasmic constituents under stress conditions. To examine whether the recombinant adenoviruses affected autophagy in MCF-7 cells, several autophagic assays were performed. Firstly, MDC staining was used to detect autophagic vacuoles. MDC is a specific dye that emits green fluorescence, which is absorbed by cells and selectively binds to autophagic vacuoles; therefore, it is known as a tracer for autophagic vesicles (34). When autophagy occurs in cells, the fluorescence of MDC staining is enhanced, and the dot-like structure (autophagic vacuoles) in a single cell is increased. Using fluorescence microscopy, it was revealed that the fluorescence intensity of MDC staining was significantly enhanced post-infection with Ad-VT or Ad-VP3, and punctate MDC-positive fluorescent particles were observed in the cytoplasm. Notably, >5 fluorescent spots were considered to indicate positive fluorescence, and 100 cells were counted to calculate the rate of autophagy. As shown in Fig. 4A, apoptin induced the accumulation of MDC-labeled vacuoles in the cytoplasm. The accumulation of autophagic corpuscles in the cytoplasm was increased in the Ad-VP3 and Ad-VT groups compared with in the control group and the Ad-MOCK group. The percentage of autophagic corpuscles in 100 MCF-7 cells after 6 h is presented.

The LC3 protein is widely distributed in cells. When autophagy occurs, LC3 accumulates on the surface of autophagosomes, and LC3-I proteins are cleaved into LC3-II proteins. In the present study, LC3 was detected using pEGFP-LC3. When autophagy is induced, the majority of autophagosomes exhibit a punctate distribution. Conversely, when autophagy is inhibited, GFP-LC3 diffuses throughout the cell. Therefore, transfected GFP plasmid was used to observe the aggregation

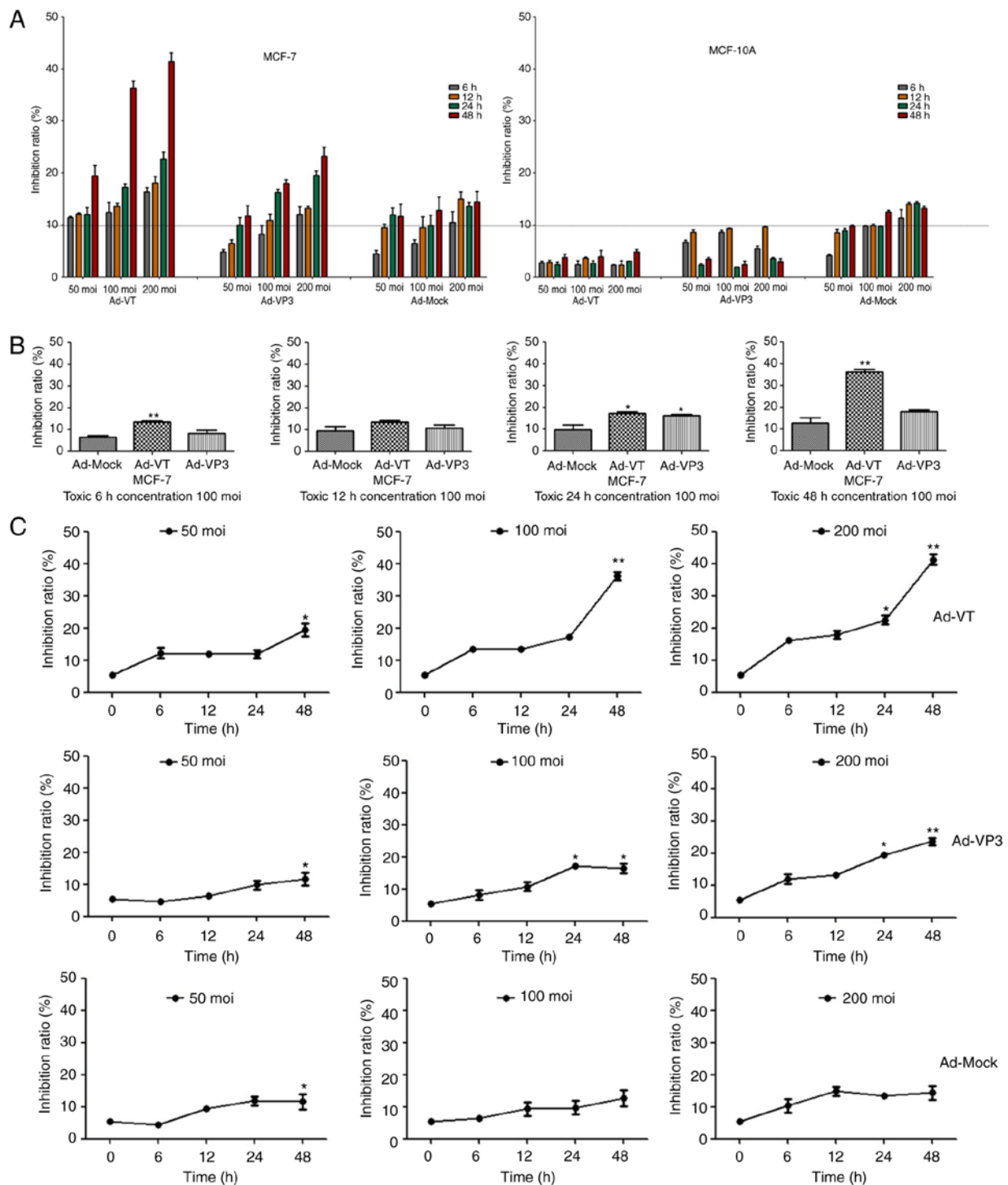


Figure 2. Recombinant adenoviruses inhibited the proliferation of MCF-7 cells. (A) MCF-10A and MCF-7 cell viability was determined using the WST-1 assay post-infection with various concentrations of Ad-VT, Ad-VP3 and Ad-MOCK (50, 100, and 200 MOI) for 6, 12, 24 and 48 h. (B) MCF-7 cell viability was determined using WST-1 assay after post-infection with Ad-VT, Ad-VP3 and Ad-MOCK (100 MOI) for various durations (6, 12, 24 and 48 h). Data are presented as the means \pm standard deviation, representative of three independent experiments ($n=3$). * $P<0.05$, ** $P<0.01$, compared with Ad-MOCK. (C) MCF-7 cell viability was determined using the WST-1 assay post-infection with various MOIs of Ad-VT, Ad-VP3 and Ad-MOCK for different durations (6, 12, 24 and 48 h). Data are presented as the means \pm standard deviation, representative of three independent experiments ($n=3$). * $P<0.05$, ** $P<0.01$, compared with the control (0 h). Ad-VP3, Ad-Apoptin; Ad-VT, Ad-Apoptin-hTERTp-E1a; MOI, multiplicity of infection.

of GFP, in order to determine whether alterations in autophagy had occurred. Ad-VT and Ad-VP3 were tested at three concentrations (50, 100, and 200 MOI) for 6 h. No obvious green fluorescent spots were detected in the cells infected with Ad-VT and Ad-VP3 at 50 MOI. Green fluorescent dot aggregation in the 100 and 200 MOI groups was obvious,

and the number of aggregated GFP points was increased in a concentration-dependent manner. Ad-VT and Ad-VP3 at 200 MOI exhibited the most obvious punctate green fluorescence. Conversely, GFP staining in the negative control group was diffuse. These results indicated that the recombinant adenoviruses could cause marked alterations in autophagy in

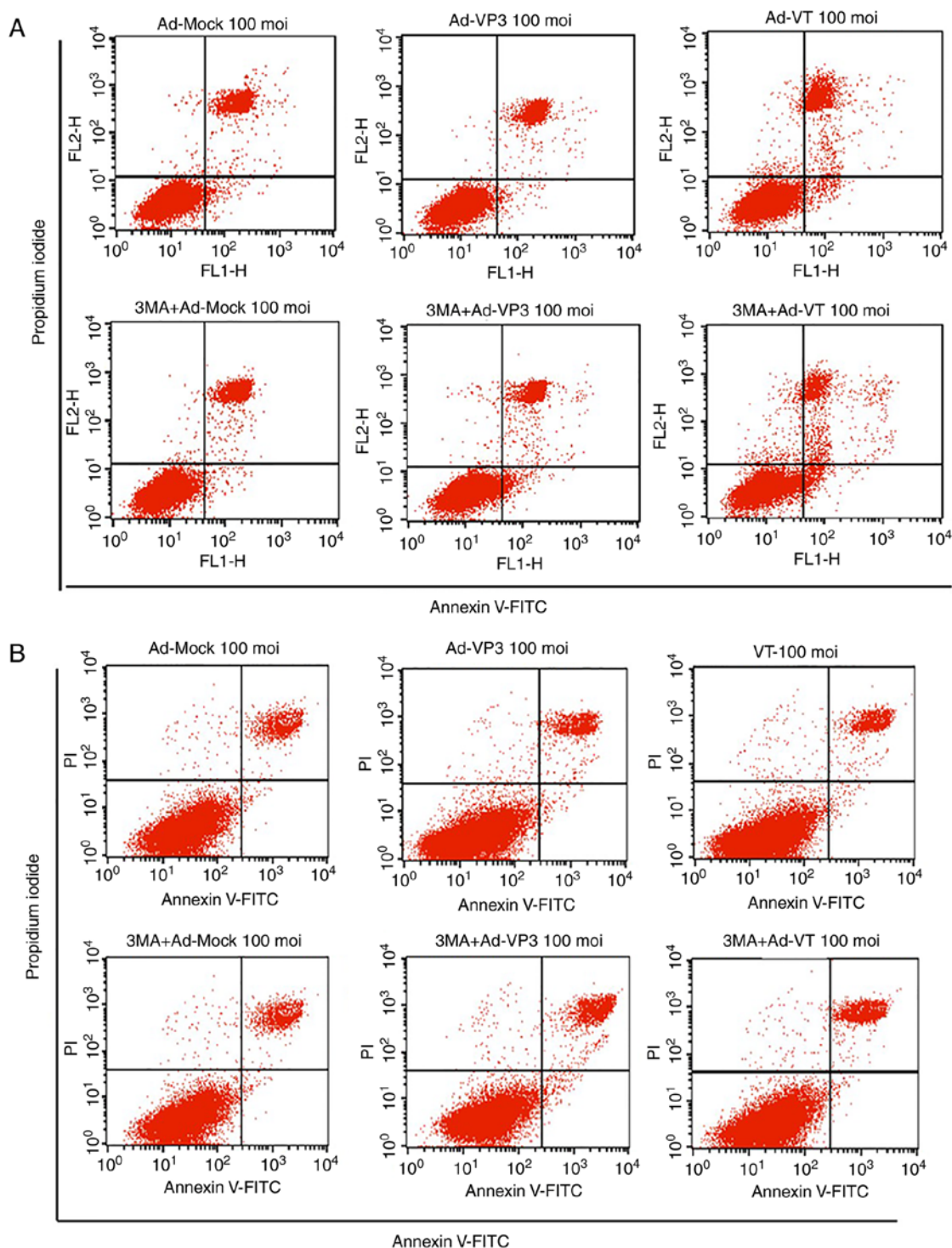


Figure 3. Analysis of cell death and cell cycle distribution of MCF-7 cells. (A) Scatter plot of Annexin V-FITC/PI staining, which was used to evaluate apoptosis of MCF-7 cells infected with Ad-VT and Ad-VP3 (100 MOI), in the presence or absence 3-MA for 24 h. (B) Scatter plot of Annexin V-FITC/PI staining, which was used to evaluate apoptosis of MCF-10A cells infected with Ad-VT and Ad-VP3 (100 MOI), in the presence or absence of 3-MA for 24 h.

MCF-7 cells, in a concentration-dependent manner (Fig. 4B). Similarly, an indirect immunofluorescence assay using fluorescence microscopy was conducted to detect the autophagy marker protein LC3-II; the present study also verified that Ad-VT and Ad-VP3 increased the expression levels of the key protein LC3-II (Fig. 4C).

TEM observation assays. TEM is the gold standard for detecting autophagosome formation, since autophagosomes have

a characteristic double membrane or multi-membrane structures. These structures were notably accumulated in MCF-7 cells infected with 100 MOI Ad-VT and Ad-VP3, indicating the formation of autophagosomes (Fig. 4D). As shown in the electron micrographs, markedly more autophagic vesicles containing subcellular materials were observed following Ad-VT and Ad-VP3 infection for 6 h compared with in the control group. The size of the autophagic vacuoles containing remnants of organelles was $\sim 2 \mu\text{m}$ in diameter.

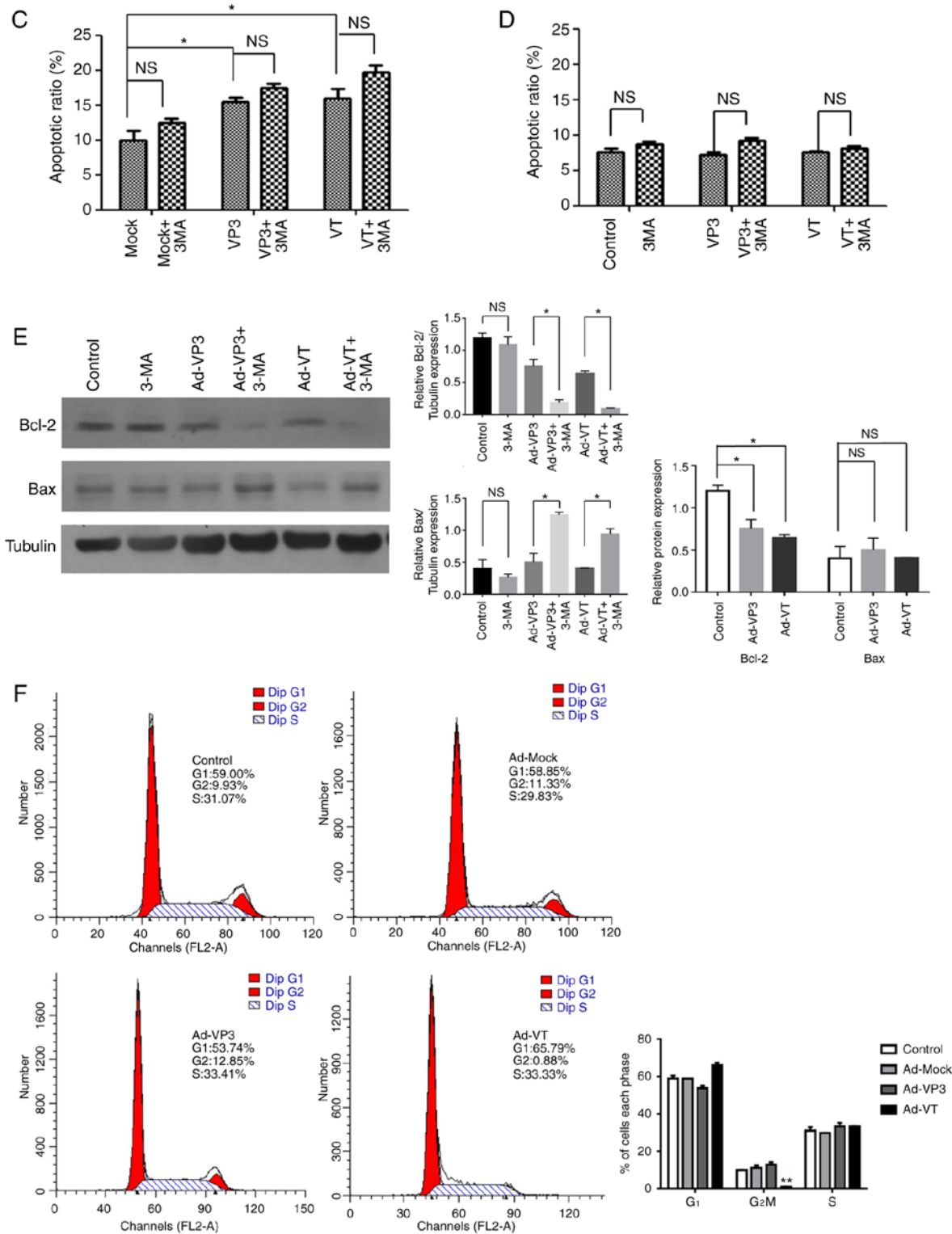


Figure 3. Continued. Analysis of cell death and cell cycle distribution of MCF-7 cells. (C) Apoptotic ratio, using Annexin V-FITC/PI staining, which was used to evaluate apoptosis of MCF-7 cells infected with Ad-VT and Ad-VP3 (100 MOI), in the presence or absence 3-MA for 24 h. (D) Apoptotic ratio, using Annexin V-FITC/PI staining, to evaluate apoptosis of MCF-10A cells infected with Ad-VT and Ad-VP3 (100 MOI), in the presence or absence of 3-MA for 24 h. (E) Western blotting of MCF-7 cell extracts for Bcl-2 and Bax. MCF-7 cells were infected with Ad-VT and Ad-VP3 (100 MOI) alone, or, after 2 h treatment with 3-MA, Ad-VT and Ad-VP3 was added to the cells for 12 h. (F) Flow cytometric analysis of cell cycle distribution of MCF-7 cells, illustrating the effects of infection with Ad-VT, Ad-VP3 and Ad-MOCK (100 MOI) for 24 h. Data are presented as the means \pm standard deviation, representative of three independent experiments (n=3). * $P < 0.05$, ** $P < 0.01$, compared with Ad-MOCK. Ad-VP3, Ad-Apoptin; Ad-VT, Ad-Apoptin-hTERTp-E1a; Bax, Bcl-2-associated X protein; Bcl-2, B-cell lymphoma 2; FITC, fluorescein isothiocyanate; MOI, multiplicity of infection; PI, propidium iodide.

Alterations in autophagy at the mRNA level. The results of the RT-qPCR analysis demonstrated that the recombinant adenoviruses induced significant alterations in autophagy in

MCF-7 cells. The results revealed that the mRNA expression levels of the autophagy-associated proteins LC3 and Beclin-1 were increased after 6 and 12 h of infection with Ad-VT

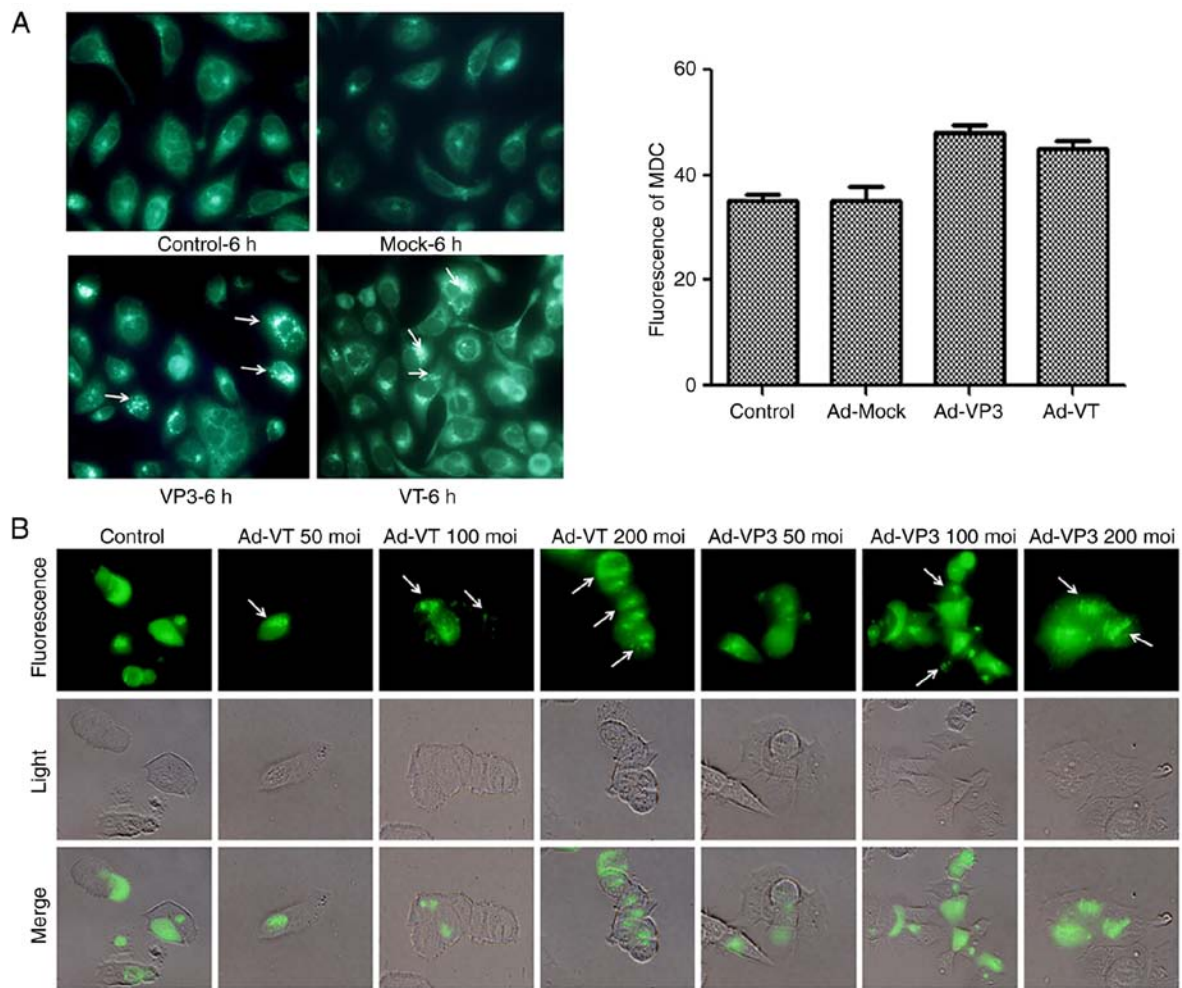


Figure 4. Apoptin induces autophagy in MCF-7 cells. (A) To evaluate autophagic vacuoles, MCF7 cells were infected with Ad-MOCK, Ad-VT, and Ad-VP3 (100 MOI) for 6 h and stained with MDC. The graph shows the percentage of MDC-stained autophagic corpuscles in MCF-7 cells in the various groups after 6 h (magnification, $\times 40$). (B) MCF-7 cells were transfected with pEGFP-LC3B for 24 h and then infected with various concentrations Ad-VT or Ad-VP3 (50, 100, and 200 MOI) for 6 h. pEGFP-LC3 signals were observed by fluorescence microscopy (magnification, $\times 40$).

and Ad-VP3. In particular, LC3 expression was significantly increased after 6 h ($P < 0.001$; Fig. 5A). After 24 h, the expression levels of LC3 and Beclin-1 were decreased compared with in the blank control group. After 48 h, the expression levels of Beclin-1 were markedly increased again, whereas LC3 exhibited the opposite trend (Fig. 5A). In addition, post-infection with Ad-VP3, the mRNA expression levels of P62 exhibited the opposite trend to LC3 at different time periods (Fig. 5A).

Alterations in autophagy at the protein level. The results of western blotting also indicated that the expression levels of LC3-II were increased in response to 100 MOI Ad-VT and Ad-VP3 compared with 1 and 10 MOI adenoviruses (Fig. 5B). The amount of LC3-II has been reported to be proportional to the number of autophagic vacuoles (35). In the present study, the ratio of LC3-II/I gradually decreased from 6 h and reached its lowest point at 48 h (Fig. 5B). Beclin-1 protein expression was not significantly altered in response to Ad-VT and Ad-VP3 (Fig. 5C). P62 is a polyubiquitin-binding protein that contains an LC3-interacting motif and ubiquitin-binding domain. By linking ubiquitinated substrates with the autophagic machinery, P62 is incorporated into complete autophagosomes and is then degraded in autolysosomes, together with its bound

proteins (36). Therefore, protein levels of P62 show the opposite trend to the protein levels of LC3. At 6 h, this phenomenon was noticeable in the present study (Fig. 5B and D). Therefore, it may be hypothesized that at 6 h, infection of MCF-7 tumor cells with Ad-VT and Ad-VP3 may promote autophagy. It was suggested that apoptin-induced autophagy may be closely related to the autophagy pathway involving the LC3 protein, and may also be associated with Beclin-1 and P62 protein levels.

Proteomics analysis of the pathways involved in apoptin-induced autophagy. Post-infection of MCF-7 cells with recombinant adenoviruses, the quantity of numerous proteins was altered compared with in the control group (Fig. 6). The present study focused on the upregulated and downregulated proteins (marked by a red arrow in Fig. 6A). The results of cluster analysis revealed that for total protein abundance, 48 h Ad-VT and 48 h Ad-VP3 were initially clustered together, which were then clustered together with 6 h Ad-VP3 and finally clustered with 6 h Ad-VT. These findings indicated that the total protein abundance of the 48 h Ad-VT and 48 h Ad-VP3 samples were relatively closer than the total protein abundance of the 6 h Ad-VT and 6 h Ad-VP3 samples. With regards to

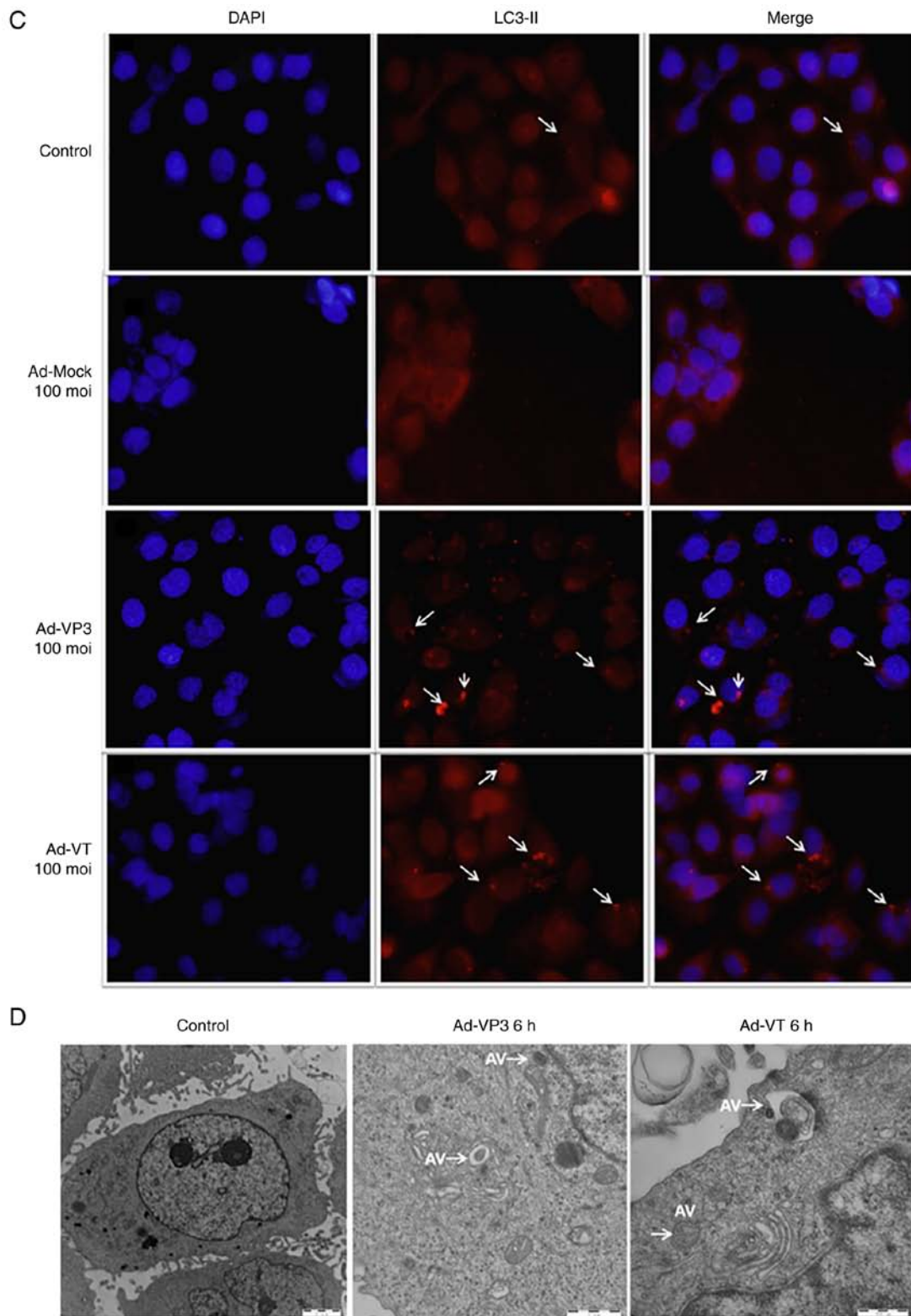


Figure 4. Continued. Apoptin induces autophagy in MCF-7 cells. (C) Representative images of immunocytochemistry. Visualization of LC3 by fluorescence microscopy. MCF-7 cells were infected with Ad-MOCK, Ad-VT and Ad-VP3 (100 MOI) for 6 h and stained with an antibody recognizing LC3 for 18 h post-treatment. The control cells exhibited diffuse cytosolic LC3 distribution. Ad-VP3-infected cells exhibited an increase in the number of cells with LC3 dots, whereas the number of cells with LC3 dots was further increased upon Ad-VT exposure. Red fluorescence indicates the presence of the LC3 protein (magnification, x40). (D) Transmission electron microscopy revealed autophagosome ultrastructures in the enlarged images following infection of cells with Ad-VT or Ad-VP3 for 6 h. Control: magnification, x5,000; Ad-VT and Ad-VP3: magnification, x10,000. Ad-VP3, Ad-Apoptin; Ad-VT, Ad-Apoptin-hTERTp-E1a; LC3, microtubule-associated protein 1A/1B-light chain 3; MDC, monodansylcadaverine; MOI, multiplicity of infection; pEGFP-LC3, enhanced green fluorescence protein-LC3 plasmid.

levels of phosphorylation, 6 h Ad-VT and 6 h Ad-VP3 were initially clustered together, which were then clustered with

48 h Ad-VP3 and finally clustered with 48 h Ad-VT. These findings indicated that the phosphorylation modification levels

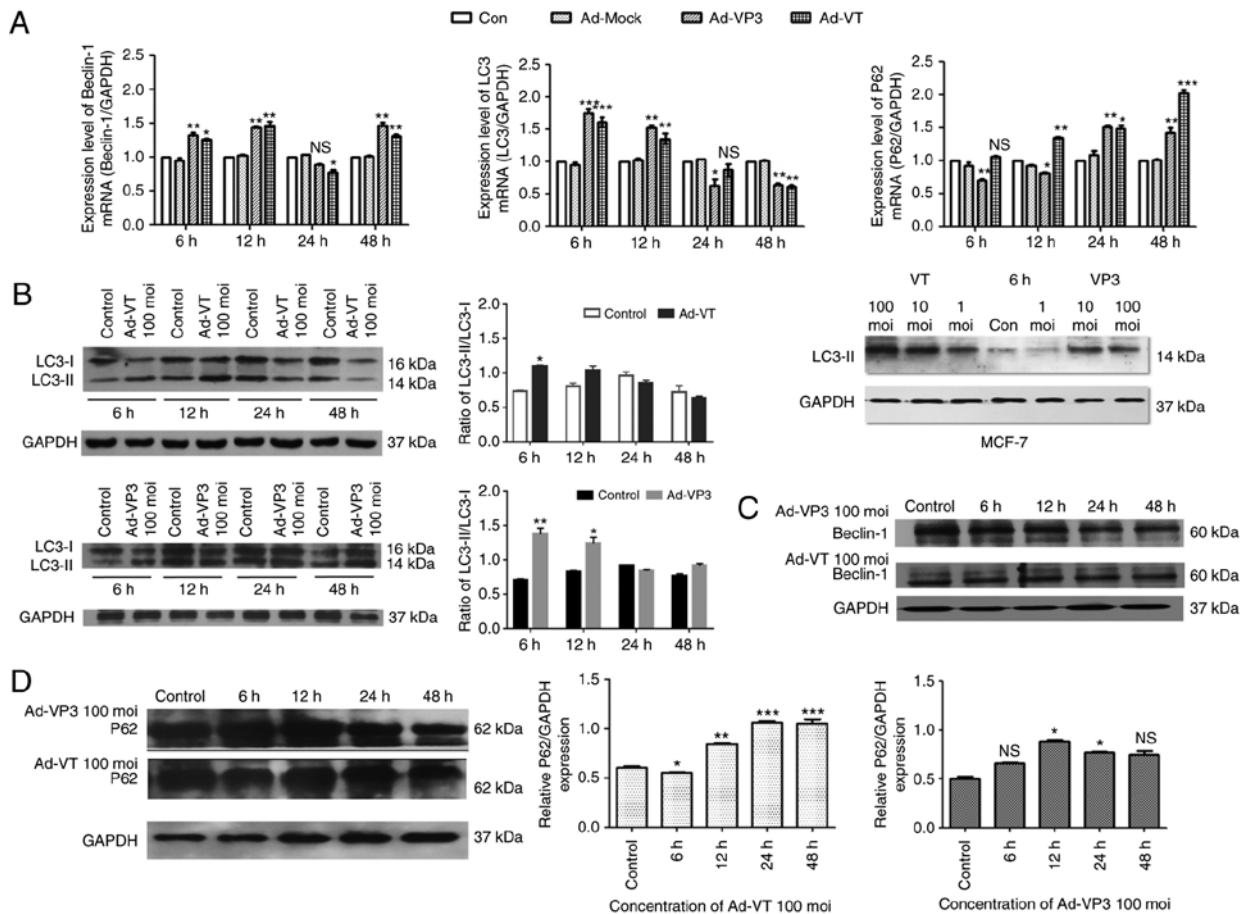


Figure 5. RT-qPCR and western blotting of MCF-7 cell extracts. GAPDH was used as a loading control. (A) Ad-VT and Ad-VP3 inhibited autophagy-mediated gene expression. The mRNA expression level of the genes encoding Beclin-1, LC3 and P62 were detected in MCF-7 cells using RT-qPCR. (B) Western blot analysis of LC3 expression in MCF-7 cells following infection with adenoviruses at various durations (6, 12, 24 and 48 h), or with different concentrations of adenoviruses (1, 10, and 100 MOI) for 6 h. (C) Western blot analysis of Beclin-1 expression in MCF-7 cells. (D) Western blot analysis of P62 expression in MCF-7 cells. Data are presented as the means \pm standard deviation, $n=3$. * $P<0.05$, ** $P<0.01$, *** $P<0.001$ vs. the control group. Ad-VP3, Ad-Apoptin; Ad-VT, Ad-Apoptin-hTERTp-E1a; LC3, microtubule-associated protein 1A/1B-light chain 3; MOI, multiplicity of infection; RT-qPCR, reverse transcription-quantitative polymerase chain reaction.

of the 6 h Ad-VT and 6 h Ad-VP3 samples were closer than the phosphorylation modification levels of the of the 48 h Ad-VT and 48 h Ad-VP3 samples. Therefore, it may be suggested that the recombinant adenovirus Ad-VP3, which only contains apoptin, promoted autophagy at 6 h in MCF-7 tumor cells via the same activation pathway as Ad-VT, which contains apoptin plus the tumor-specific promoter hTERT. These findings are mainly due to the effect of apoptin on tumor cells (Fig. 6B). In addition, the elevated proteins in the autophagy pathway were identified by KEGG (Fig. 6D) and were further verified using western blotting. The results revealed that ATG4B, ATG5 and BIF-1 (Fig. 6C), and LC3 (Fig. 5C) were markedly increased, and the levels of phosphorylated ATG4 and synaptosome associated protein 29 (SNAP29) were obviously increased (Fig. 6C and D).

Discussion

Autophagy is a process of self-degradation that may serve a dual role in cancer as a way of inducing cell death. Autophagy can inhibit cancer in the early stages, and can lead to drug resistance in cancer cells in the late stage (37-39). Increasing evidence has suggested that autophagy and apoptosis can

be synergistic or antagonistic in determining cell fate. The observed cancer-selective toxicity of apoptin (4,40) has intrigued researchers, as this viral protein targets the molecular basis of the transformed phenotype. Targeted cancer therapies interfere with malignant cell growth and division at various points during the development, growth and spread of cancer. The present study examined the effects of apoptin on MCF-7 human breast cancer cells and MCF-10A normal mammary epithelial cells. The present study investigated whether recombinant adenoviruses expressing apoptin could affect autophagy in MCF-7 human breast cancer cells. Firstly, the results revealed that infection with adenoviruses containing apoptin led to significant apoptosis of MCF-7 cells, as verified by Annexin V-FITC/PI staining, which has also been observed in another study (41). However, these adenoviruses had no effect on MCF-10A normal mammary gland cells. In addition, Ad-VT only induced G_1 arrest in MCF-7 human breast cancer cells, whereas Ad-VP3 and Ad-MOCK had no significant effect on cell cycle progression.

In the present study two apoptin-containing recombinant adenoviruses, Ad-VT and Ad-VP3, were constructed. In Ad-VT, apoptin was stably and highly expressed and the tumor specific promoter hTERT was also expressed in a human type

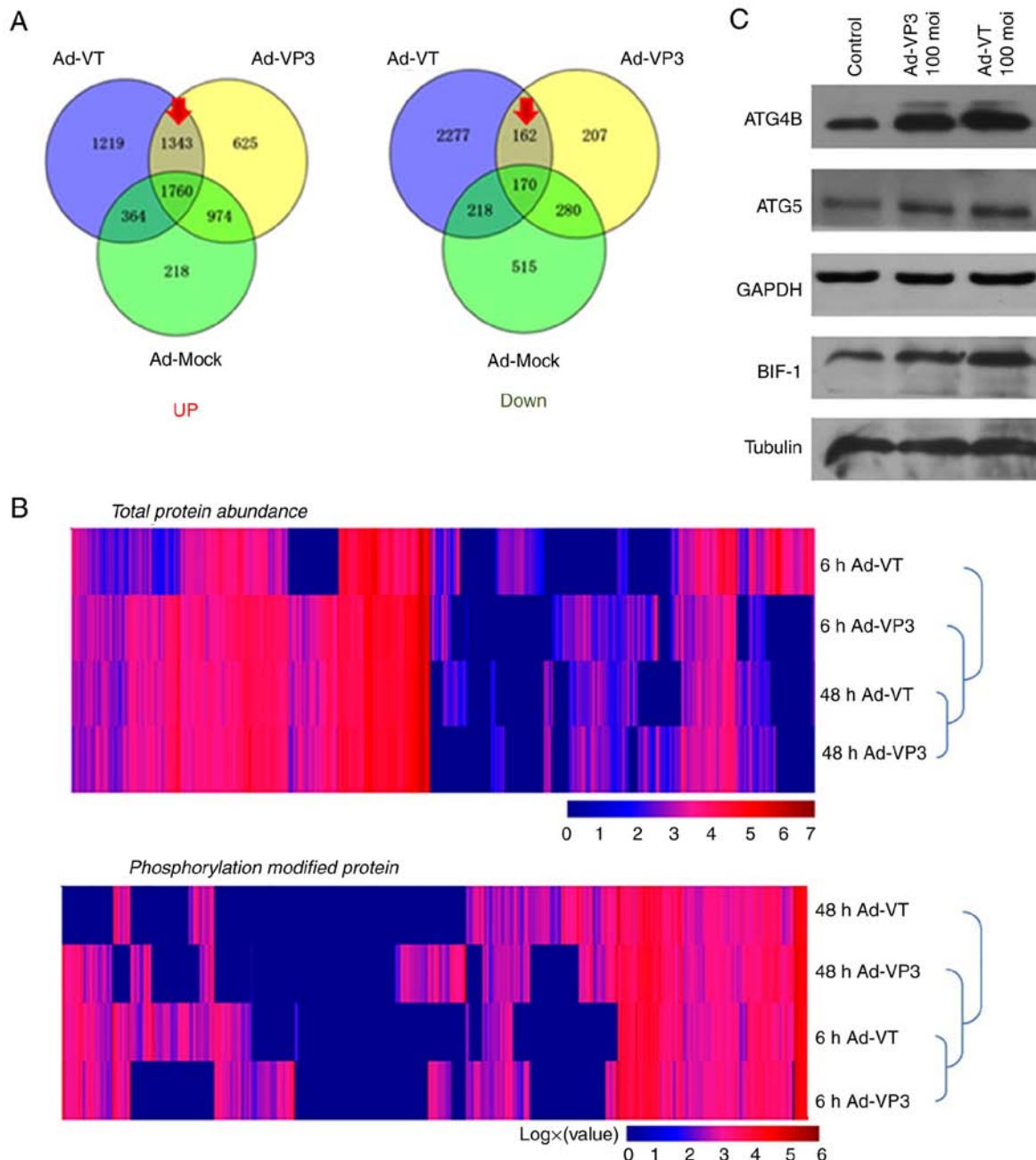


Figure 6. Proteomics confirmed that apoptin induces autophagy in MCF-7 cells. (A) Venn diagrams illustrating the identification of all proteins in MCF-7 cells. (B) Hierarchical clustering of unbiased total protein expression and hierarchical clustering of phosphorylated proteins. The pathways identified by proteomics suggested that apoptin induces autophagy. (C) Protein expression levels of ATG4b, ATG5 and BIF-1 were detected using western blotting.

5 adenovirus; therefore, Ad-VT can replicate in tumor cells. Conversely, Ad-VP3 did not have the ability to continuously replicate in cells, since it only contained apoptin. In the process of autophagy, a phagophore from the endoplasmic reticulum or plasma membrane forms autophagosomes, which depend on Beclin-1 and LC3-II (42,43). In the present study, the formation of autophagosomes was determined by TEM, and autophagic vesicles containing subcellular materials were observed post-infection with Ad-VT and Ad-VP3 for 6 h. In addition, an increase in Beclin-1 and LC3-II protein levels and a decrease in P62 protein levels was observed by RT-qPCR and western blotting, particularly post-infection with Ad-VP3 at 6 h. Autophagy decreased cell survival by destroying the cytosol and organelles, leading to cell death. In

addition, proteomics analysis revealed a significant increase in the phosphorylation of ATG4B in response to apoptin. The biosynthesis of autophagosomes involves two successive steps, one involving ATG12-ATG5 and the other involving ATG8-phosphatidyl-ethanolamine (PE) (44,45). For the latter, the ATG4 cysteine protease cleaves the newly synthesized ATG8 to reveal glycine residues and membrane-bound PE (lipid binding) binding. ATG4 can also remove PE from ATG8 (delipidation). In humans, LC3B is the best characteristic ATG8 subtype (44,46-48). In addition, ATG4B, but not three other ATG4 subtypes, exhibit a highly selective preference for LC3B (49). A mouse model of genetic engineering was used to study the importance of ATG4B in normal development and disease. The results indicated that an ATG4B deficiency may

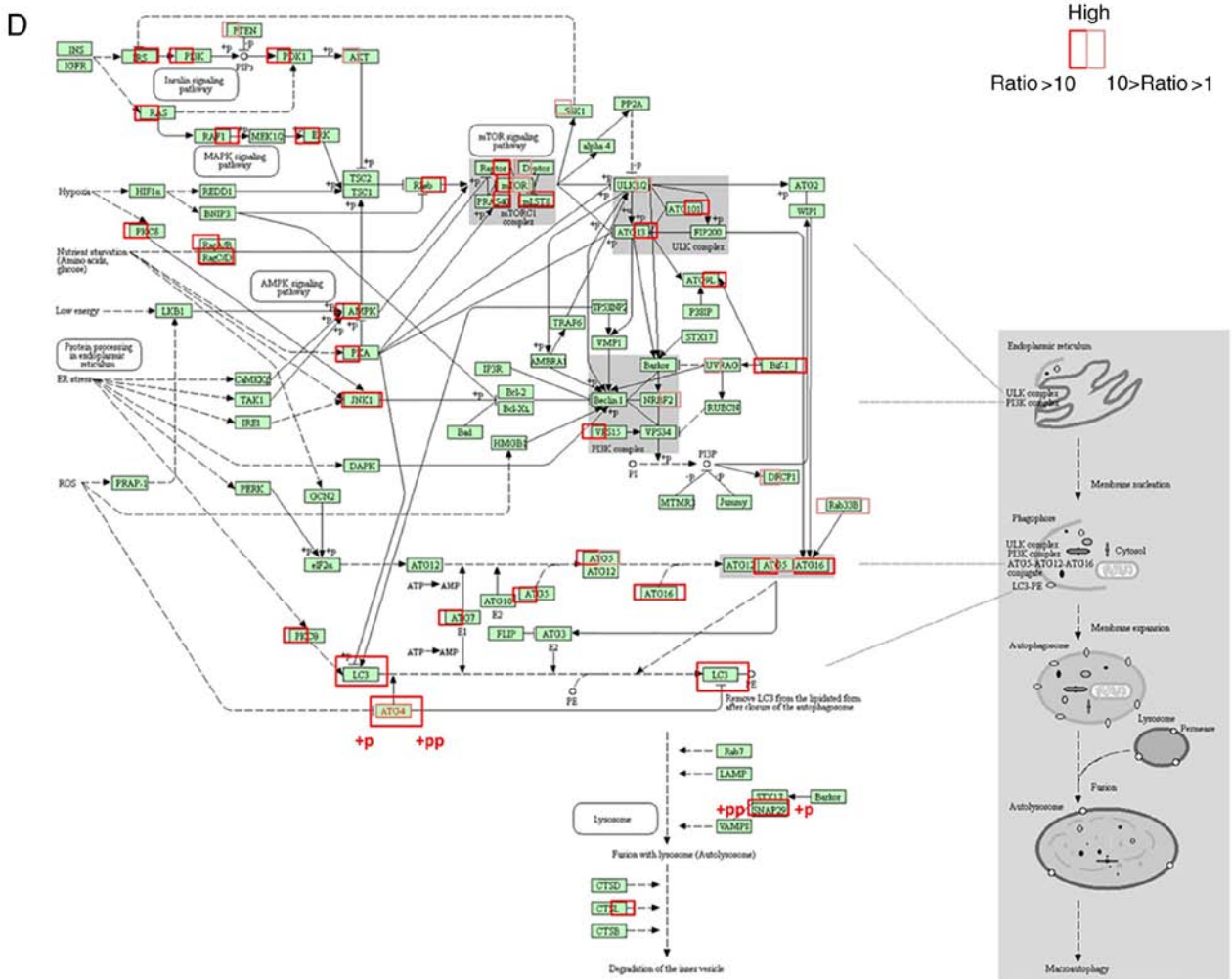


Figure 6. Continued. Proteomics confirmed that apoptin induces autophagy in MCF-7 cells. (D) Proteomic data revealed components of the autophagy signaling pathways. Proteins more abundant in Ad-VT-infected MCF-7 cells are shown in red (the ratio of Ad-VT/control was >10) and those that are a little more abundant in Ad-VT-infected MCF-7 cells are shown in pink (the ratio of Ad-VT/control was >1, but <10). Markedly elevated proteins are surrounded by a frame, indicating an increase in expression following Ad-VT and Ad-VP3 stimulation; when the left-hand side of the protein is framed this represents an increase in response to Ad-VT stimulation compared with the control group, whereas when the right-hand side of the protein is framed this represents an increase in response to Ad-VP3 compared with the control group. +p and +pp indicate the degree of phosphorylated protein expression; compared with the control group, +pp is more significant than +p. Ad-VP3, Ad-Apoptin; Ad-VT, Ad-Apoptin-hTERTp-E1a; MOI, multiplicity of infection.

lead to a reduction in autophagy (50). In cancer, ATG4B and LC3 have been implicated with the regulation of autophagy, as a biomarker and potential therapeutic target.

Apoptosis and autophagy are two different forms of cell death, which are independent of each other and restrict each other. Numerous genes serve an important role in the mutual transformation of the two different forms, including Beclin-1 and Bcl-2. Members of the Bcl-2 family have an important role in the regulation of mammalian cell apoptosis, targeting upstream of irreversible cell damage, and working primarily at the mitochondrial level. According to the structure and function of family members, they are divided into anti-apoptotic proteins, including Bcl-2 and Bcl-extra large, and proapoptotic proteins, including Bax. A recent study revealed that dihydroartemisinin has antitumor activity in cholangiocarcinoma and can reduce the interaction of Beclin-N1 with Bcl-2 while promoting its interaction with Phosphatidylinositol 3-kinase catalytic subunit type 3 (51). Similar results were revealed in the present study. To investigate the role of apoptin-induced autophagy in apoptosis, the autophagy-specific inhibitor 3-MA

was used to suppress autophagy and to investigate the relationship between autophagy and apoptosis in MCF-7 cells. It has previously been reported that the autophagy inhibitor 3-MA can enhance endoplasmic reticulum stress-induced apoptosis of nasopharyngeal carcinoma cells (52). In the present study, western blotting results revealed that the expression levels of the apoptosis-associated protein Bcl-2 were significantly decreased when Ad-VP3 or Ad-VT infection was combined with 3-MA treatment, whereas the expression levels of the proapoptotic protein Bax were significantly increased. There was no significant difference between cells treated with 3-MA alone and the control group. Therefore, it was hypothesized that inhibition of autophagy could increase the apoptosis of MCF-7 cells infected with recombinant adenoviruses.

To the best of our knowledge, the present study is the first to reveal that recombinant adenoviruses expressing apoptin may significantly affect autophagy in MCF-7 breast cancer cells. The results indicated that the recombinant adenoviruses may enhance protective autophagy at the early stage (6 h) in MCF-7 breast cancer cells, such that cell damage by apoptosis

is inhibited. However, with the prolongation of apoptin treatment duration, autophagy began to decrease. It was therefore hypothesized that apoptosis may gradually dominate following extended treatment with apoptin. It remains to be determined how apoptin interacts with autophagy and apoptosis of MCF-7 cells. In conclusion, the present study demonstrated that recombinant adenoviruses expressing apoptin inhibited the early growth of breast cancer cells via a mechanism associated with the induction of autophagy. Our future study aims to analyze more breast cancer cell lines alongside mammary epithelial cells as a control. These results may lead to novel strategies to prevent and treat breast cancer.

Acknowledgements

Not applicable.

Funding

This study was supported by the National Key Research and Development Program of China (grant no. 2016YFC1200900) and the Major Technological Program of Changchun City (grant no. 16ss11).

Availability of data and materials

All data generated or analyzed during this study are included in this published article.

Authors' contributions

NYJ and XL designed the study and provided funding. QGZ coordinated the study. SC designed and performed the experiments, and analyzed the data. YQL, XZY, YLZ, YYF, WJL, SZL, YLC and JZ performed the experiments. SC wrote the manuscript. QGZ and YQL participated in editing the manuscript. QGZ was involved in the conception and design of the study. All authors reviewed the results and approved the final version of the manuscript.

Ethics approval and consent to participate

Not applicable.

Patient consent for publication

Not applicable.

Competing interests

The authors declare that they have no competing interests.

References

- Noteborn MH, de Boer GF, van Roozelaar DJ, Karreman C, Kranenburg O, Vos JG, Jeurissen SH, Hoeben RC, Zantema A and Koch G: Characterization of cloned chicken anemia virus DNA that contains all elements for the infectious replication cycle. *J Virol* 65: 3131-3139, 1991.
- Noteborn MH and Koch G: Chicken anaemia virus infection: Molecular basis of pathogenicity. *Avian Pathol* 24: 11-31, 1995.
- Noteborn MH, Todd D, Verschuere CA, de Gauw HW, Curran WL, Veldkamp S, Douglas AJ, McNulty MS, van der Eb AJ and Koch G: A single chicken anemia virus protein induces apoptosis. *J Virol* 68: 346-351, 1994.
- Danen-Van Oorschot AA, Fischer DF, Grimbergen JM, Klein B, Zhuang S, Falkenburg JH, Backendorf C, Quax PH, van der Eb AJ and Noteborn MH: Apoptin induces apoptosis in human transformed and malignant cells but not in normal cells. *Proc Natl Acad Sci USA* 94: 5843-5847, 1997.
- Guelen L, Paterson H, Gäken J, Meyers M, Farzaneh F and Tavassoli M: TAT-apoptin is efficiently delivered and induces apoptosis in cancer cells. *Oncogene* 23: 1153-1165, 2004.
- Pietersen AM, van der Eb MM, Rademaker HJ, van den Wollenberg DJ, Rabelink MJ, Kuppen PJ, van Dierendonck JH, van Ormondt H, Masman D, van de Velde CJ, *et al*: Specific tumor-cell killing with adenovirus vectors containing the apoptin gene. *Gene Ther* 6: 882-892, 1999.
- Zhuang SM, Landegent JE, Verschuere CA, Falkenburg JH, van Ormondt H, van der Eb AJ and Noteborn MH: Apoptin, a protein encoded by chicken anemia virus, induces cell death in various human hematologic malignant cells in vitro. *Leukemia* 9 (Suppl 1): S118-S120, 1995.
- Greider CW: Telomere length regulation. *Annu Rev Biochem* 65: 337-365, 1996.
- Shay JW and Bacchetti S: A survey of telomerase activity in human cancer. *Eur J Cancer* 33: 787-791, 1997.
- Takakura M, Kyo S, Kanaya T, Hirano H, Takeda J, Yutsudo M and Inoue M: Cloning of human telomerase catalytic subunit (hTERT) gene promoter and identification of proximal core promoter sequences essential for transcriptional activation in immortalized and cancer cells. *Cancer Res* 59: 551-557, 1999.
- Kyo S, Takakura M, Taira T, Kanaya T, Itoh H, Yutsudo M, Ariga H and Inoue M: Sp1 cooperates with c-Myc to activate transcription of the human telomerase reverse transcriptase gene (*hTERT*). *Nucleic Acids Res* 28: 669-677, 2000.
- Li X, Liu Y, Wen Z, Li C, Lu H, Tian M, Jin K, Sun L, Gao P, Yang E, *et al*: Potent anti-tumor effects of a dual specific oncolytic adenovirus expressing apoptin in vitro and in vivo. *Mol Cancer* 9: 10, 2010.
- Liu L, Wu W, Zhu G, Liu L, Guan G, Li X, Jin N and Chi B: Therapeutic efficacy of an hTERT promoter-driven oncolytic adenovirus that expresses apoptin in gastric carcinoma. *Int J Mol Med* 30: 747-754, 2012.
- Zhang M, Wang J, Li C, Hu N, Wang K, Ji H, He D, Quan C, Li X, Jin N, *et al*: Potent growth-inhibitory effect of a dual cancer-specific oncolytic adenovirus expressing apoptin on prostate carcinoma. *Int J Oncol* 42: 1052-1060, 2013.
- Qi Y, Guo H, Hu N, He D, Zhang S, Chu Y, Huang Y, Li X, Sun L and Jin N: Preclinical pharmacology and toxicology study of Ad-hTERT-E1a-Apoptin, a novel dual cancer-specific oncolytic adenovirus. *Toxicol Appl Pharmacol* 280: 362-369, 2014.
- Yang G, Meng X, Sun L, Hu N, Jiang S, Sheng Y, Chen Z, Zhou Y, Chen D, Li X, *et al*: Antitumor effects of a dual cancer-specific oncolytic adenovirus on colorectal cancer in vitro and in vivo. *Exp Ther Med* 9: 327-334, 2015.
- Watanabe E, Muenzer JT, Hawkins WG, Davis CG, Dixon DJ, McDunn JE, Brackett DJ, Lerner MR, Swanson PE and Hotchkiss RS: Sepsis induces extensive autophagic vacuolization in hepatocytes: A clinical and laboratory-based study. *Lab Invest* 89: 549-561, 2009.
- Mukhopadhyay S, Panda PK, Sinha N, Das DN and Bhutia SK: Autophagy and apoptosis: Where do they meet? *Apoptosis* 19: 555-566, 2014.
- Kubisch J, Türei D, Földvári-Nagy L, Dunai ZA, Zsákai L, Varga M, Vellai T, Csermely P and Korcsmáros T: Complex regulation of autophagy in cancer-integrated approaches to discover the networks that hold a double-edged sword. *Semin Cancer Biol* 23: 252-261, 2013.
- Kim Y, Jeong IG, You D, Song SH, Suh N, Jang SW, Kim S, Hwang JJ and Kim CS: Sodium meta-arsenite induces reactive oxygen species-dependent apoptosis, necrosis, and autophagy in both androgen-sensitive and androgen-insensitive prostate cancer cells. *Anticancer Drugs* 25: 53-62, 2014.
- Shen S, Kepp O and Kroemer G: The end of autophagic cell death? *Autophagy* 8: 1-3, 2012.
- Denton D, Xu T and Kumar S: Autophagy as a pro-death pathway. *Immunol Cell Biol* 93: 35-42, 2015.
- Berry DL and Baehrecke EH: Autophagy functions in programmed cell death. *Autophagy* 4: 359-360, 2008.

24. Maiuri MC, Zalckvar E, Kimchi A and Kroemer G: Self-eating and self-killing: Crosstalk between autophagy and apoptosis. *Nat Rev Mol Cell Biol* 8: 741-752, 2007.
25. Shen HM and Codogno P: Autophagic cell death: Loch Ness monster or endangered species? *Autophagy* 7: 457-465, 2011.
26. Lum JJ, Bauer DE, Kong M, Harris MH, Li C, Lindsten T and Thompson CB: Growth factor regulation of autophagy and cell survival in the absence of apoptosis. *Cell* 120: 237-248, 2005.
27. Amaravadi RK and Thompson CB: The roles of therapy-induced autophagy and necrosis in cancer treatment. *Clin Cancer Res* 13: 7271-7279, 2007.
28. Wu YT, Tan HL, Huang Q, Kim YS, Pan N, Ong WY, Liu ZG, Ong CN and Shen HM: Autophagy plays a protective role during zVAD-induced necrotic cell death. *Autophagy* 4: 457-466, 2008.
29. Guo JY, Chen HY, Mathew R, Fan J, Strohecker AM, Karsli-Uzunbas G, Kamphorst JJ, Chen G, Lemons JM, Karantza V, *et al*: Activated Ras requires autophagy to maintain oxidative metabolism and tumorigenesis. *Genes Dev* 25: 460-470, 2011.
30. Shimizu S, Kanaseki T, Mizushima N, Mizuta T, Arakawa-Kobayashi S, Thompson CB and Tsujimoto Y: Role of Bcl-2 family proteins in a non-apoptotic programmed cell death dependent on autophagy genes. *Nat Cell Biol* 6: 1221-1228, 2004.
31. Sharifi MN, Mowers EE, Drake LE, Collier C, Chen H, Zamora M, Mui S and Macleod KF: Autophagy promotes focal adhesion disassembly and cell motility of metastatic tumor cells through the direct interaction of paxillin with LC3. *Cell Rep* 15: 1660-1672, 2016.
32. Klionsky DJ, Abdalla FC, Abeliovich H, Abraham RT, Acevedo-Arozena A, Adeli K, Agholme L, Agnello M, Agostinis P, Aguirre-Ghiso JA, *et al*: Guidelines for the use and interpretation of assays for monitoring autophagy. *Autophagy* 8: 445-544, 2012.
33. Livak KJ and Schmittgen TD: Analysis of relative gene expression data using real-time quantitative PCR and the $2^{-\Delta\Delta CT}$ method. *Methods* 25: 402-408, 2001.
34. Biederick A, Kern HF and Elsässer HP: Monodansylcadaverine (MDC) is a specific in vivo marker for autophagic vacuoles. *Eur J Cell Biol* 66: 3-14, 1995.
35. Klionsky DJ, Abdelmohsen K, Abe A, Abedin MJ, Abeliovich H, Acevedo Arozena A, Adachi H, Adams CM, Adams PD, Adeli K, *et al*: Guidelines for the use and interpretation of assays for monitoring autophagy (3rd edition). *Autophagy* 12: 1-222, 2016.
36. Saiki S, Sasazawa Y, Imamichi Y, Kawajiri S, Fujimaki T, Tanida I, Kobayashi H, Sato F, Sato S, Ishikawa K, *et al*: Caffeine induces apoptosis by enhancement of autophagy via PI3K/Akt/mTOR/p70S6K inhibition. *Autophagy* 7: 176-187, 2011.
37. Perkins ND: The diverse and complex roles of NF- κ B subunits in cancer. *Nat Rev Cancer* 12: 121-132, 2012.
38. Janku F, McConkey DJ, Hong DS and Kurzrock R: Autophagy as a target for anticancer therapy. *Nat Rev Clin Oncol* 8: 528-539, 2011.
39. Blessing AM, Rajapakshe K, Reddy Bollu L, Shi Y, White MA, Pham AH, Lin C, Jonsson P, Cortes CJ, Cheung E, *et al*: Transcriptional regulation of core autophagy and lysosomal genes by the androgen receptor promotes prostate cancer progression. *Autophagy* 13: 506-521, 2017.
40. Poon IK, Oro C, Dias MM, Zhang JP and Jans DA: A tumor cell-specific nuclear targeting signal within chicken anemia virus VP3/apoptin. *J Virol* 79: 1339-1341, 2005.
41. Shen Ni L, Allaudin ZN, Mohd Lila MA, Othman AM and Othman FB: Selective apoptosis induction in MCF-7 cell line by truncated minimal functional region of Apoptin. *BMC Cancer* 13: 488, 2013.
42. Kroemer G and Levine B: Autophagic cell death: The story of a misnomer. *Nat Rev Mol Cell Biol* 9: 1004-1010, 2008.
43. Pradhan AK, Talukdar S, Bhoopathi P, Shen XN, Emdad L, Das SK, Sarkar D and Fisher PB: *mda-7/IL-24* mediates cancer cell-specific death via regulation of miR-221 and the beclin-1 axis. *Cancer Res* 77: 949-959, 2017.
44. Mizushima N, Yoshimori T and Ohsumi Y: The role of Atg proteins in autophagosome formation. *Annu Rev Cell Dev Biol* 27: 107-132, 2011.
45. White E: The role for autophagy in cancer. *J Clin Invest* 125: 42-46, 2015.
46. Kabeya Y, Mizushima N, Yamamoto A, Oshitani-Okamoto S, Ohsumi Y and Yoshimori T: LC3, GABARAP and GATE16 localize to autophagosomal membrane depending on form-II formation. *J Cell Sci* 117: 2805-2812, 2004.
47. Tanida I, Ueno T and Kominami E: Human light chain 3/MAP1LC3B is cleaved at its carboxyl-terminal Met121 to expose Gly120 for lipidation and targeting to autophagosomal membranes. *J Biol Chem* 279: 47704-47710, 2004.
48. Klionsky DJ, Cuervo AM and Seglen PO: Methods for monitoring autophagy from yeast to human. *Autophagy* 3: 181-206, 2007.
49. Mariño G, Uría JA, Puente XS, Quesada V, Bordallo J and López-Otín C: Human autophagins, a family of cysteine proteinases potentially implicated in cell degradation by autophagy. *J Biol Chem* 278: 3671-3678, 2003.
50. Akin D, Wang SK, Habibzadegah-Tari P, Law B, Ostrov D, Li M, Yin XM, Kim JS, Horenstein N, Dunn WA Jr: A novel ATG4B antagonist inhibits autophagy and has a negative impact on osteosarcoma tumors. *Autophagy* 10: 2021-2035, 2014.
51. Thongchot S, Vidoni C, Ferraresi A, Loilome W, Yongvanit P, Namwat N and Isidoro C: Dihydroartemisinin induces apoptosis and autophagy-dependent cell death in cholangiocarcinoma through a DAPK1-BECLIN1 pathway. *Mol Carcinog* 57: 1735-1750, 2018.
52. Song L, Ma L, Zhang X, Jiang Z, Liu H and Jiang C: Effect of tunicamycin combined with cisplatin on proliferation and apoptosis of human nasopharyngeal carcinoma cells in vitro. *Nan Fang Yi Ke Da Xue Xue Bao* 32: 766-771, 2012 (In Chinese).



This work is licensed under a Creative Commons Attribution-NonCommercial-NoDerivatives 4.0 International (CC BY-NC-ND 4.0) License.